Kitaev Spin Liquid in 3*d* Transition Metal Compounds

Huimei Liu,[1] Jiří Chaloupka,[2,3] and Giniyat Khaliullin[1]
[1]Max Planck Institute for Solid State Research, Heisenbergstrasse 1, D-70569 Stuttgart, Germany
[2]Department of Condensed Matter Physics, Faculty of Science, Masaryk University, Kotlářská 2, Brno 61137, Czech Republic
[3]Central European Institute of Technology, Masaryk University, Kamenice 753/5, Brno 62500, Czech Republic

(Received 10 February 2020; accepted 2 July 2020; published 21 July 2020)

We study the exchange interactions and resulting magnetic phases in the honeycomb cobaltates. For a broad range of trigonal crystal fields acting on Co^{2+} ions, the low-energy pseudospin-1/2 Hamiltonian is dominated by bond-dependent Ising couplings that constitute the Kitaev model. The non-Kitaev terms nearly vanish at small values of trigonal field Δ, resulting in spin liquid ground state. Considering $Na_3Co_2SbO_6$ as an example, we find that this compound is proximate to a Kitaev spin liquid phase, and can be driven into it by slightly reducing Δ by $\sim$20 meV, e.g., via strain or pressure control. We argue that, due to the more localized nature of the magnetic electrons in 3*d* compounds, cobaltates offer the most promising search area for Kitaev model physics.

DOI: 10.1103/PhysRevLett.125.047201

The Kitaev honeycomb model [1], demonstrating the key concepts of quantum spin liquids [2] via an elegant exact solution, has attracted much attention (see the recent reviews [3–7]). In this model, the nearest-neighbor (NN) spins $S = 1/2$ interact via a simple Ising-type coupling $S_i^\gamma S_j^\gamma$. However, the Ising axis γ is not global but bond dependent, taking the mutually orthogonal directions (x, y, z) on the three adjacent NN bonds on the honeycomb lattice. Having no unique easy axis and being frustrated, the Ising spins fail to order and form instead a highly entangled quantum many-body state, supporting fractional excitations described by Majorana fermions [1].

Much effort has been made to realize the Kitaev spin liquid (SL) experimentally. From a materials perspective, the Ising-type anisotropy is a hallmark of unquenched orbital magnetism. As the orbitals are spatially anisotropic and bond directional, they naturally lead to the desired bond-dependent exchange anisotropy via spin-orbit coupling [8]. Along these lines, 5*d* iridates have been suggested [9] to host Kitaev model; later, 4*d* $RuCl_3$ was added [10] to the list of candidates. To date, however, the Kitaev SL remains elusive, as this state is fragile and destroyed by various perturbations, such as small admixture of a conventional Heisenberg coupling [11] caused by direct overlap of the *d* orbitals. Even more detrimental to Kitaev SL are the longer range couplings [12], unavoidable in weakly localized 5*d*- and 4*d*-electron systems with the spatially extended *d* wave functions. We thus turn to 3*d* systems with more compact *d* orbitals [13].

While the idea of extending the search area to 3*d* materials is appealing, and plausible theoretically [15,16], it raises an immediate question crucial for experiment: is spin-orbit coupling (SOC) in 3*d* ions strong enough to support the orbital magnetism prerequisite for the Kitaev model design? This is a serious concern, since noncubic crystal fields present in real materials tend to quench orbital moments and suppress the bond dependence of the exchange couplings [8]. In this Letter, we give a positive answer to this question. Our quantitative analysis of the crystal field effects on the magnetism of 3*d* cobaltates shows that the orbital moments remain active and generate a Kitaev model as the leading term in the Hamiltonian. In fact, we identify the trigonal crystal field as the key and experimentally tunable parameter, which decides the strength of the non-Kitaev terms in 3*d* compounds.

Our main results are summarized in Fig. 1, displaying various magnetic phases of spin-orbit entangled pseudospin-1/2 Co^{2+} ions on a honeycomb lattice. The phase diagram is shown as a function of trigonal field Δ, in a window relevant for honeycomb cobaltates, and a ratio of Coulomb repulsion U and the charge-transfer gap Δ_{pd} [17]. From the analysis of experimental data, we find that $Na_3Co_2SbO_6$ [18–20] is located at just $\sim$20 meV "distance" from the Kitaev SL phase (see Fig. 1), and could be driven there by a *c*-axis compression that reduces Δ. This seems feasible, given that Δ variations within a window of $\sim$70 meV were achieved by strain control in a cobalt oxide [21].

We now describe our calculations resulting in Fig. 1. In short, we first derive the pseudospin exchange interactions from a microscopic theory, as a function of various

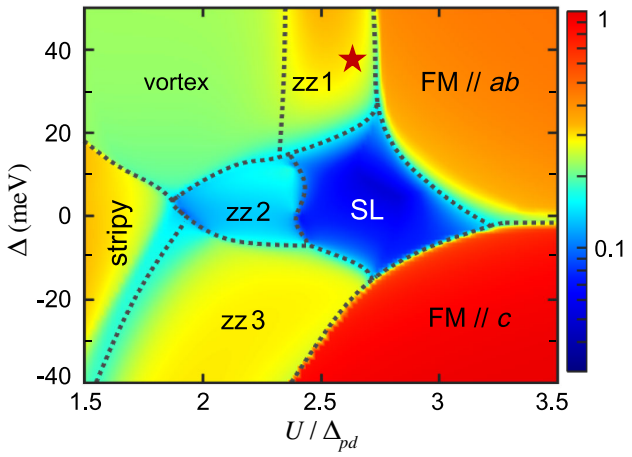

FIG. 1. The calculated magnetic phase diagram of honeycomb cobaltates. The Kitaev SL phase is surrounded by ferromagnetic (FM) states with moments in the honeycomb ab plane and along the c axis, zigzag-type states with moments in the ab plane (zz1), along Co-O bonds (zz2), and in the ac plane (zz3). Vortex- and stripy-type phases take over at smaller U/Δ_{pd}. The color map shows the second-NN spin correlation strength (leading eigenvalue of the correlation matrix $\langle \tilde{S}_i^{\alpha}\tilde{S}_j^{\beta}\rangle$ normalized by $\tilde{S}^2 = 1/4$), which drops sharply in the SL phase. The star indicates the rough position of $Na_3Co_2SbO_6$.

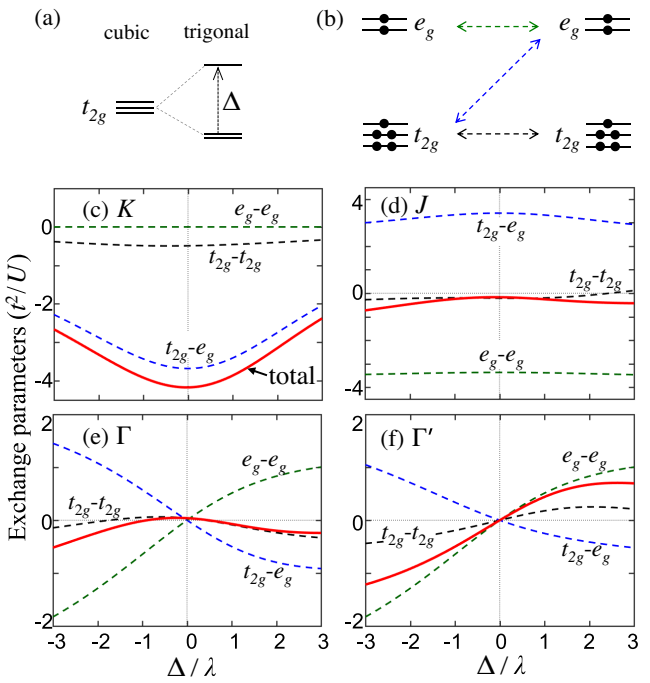

FIG. 2. (a) Splitting of t_{2g}-electron level under trigonal crystal field. (b) Schematic of the spin-orbital exchange channels for d^7 ions. (c)–(f) Exchange parameters K, J, Γ, and Γ' (red solid lines) as a function of Δ/λ, calculated at $U/\Delta_{pd} = 2.5$ and Hund's coupling $J_H = 0.15U$. On each panel, dashed lines show individual contributions of t_{2g}-t_{2g} (black), t_{2g}-e_g (blue), and e_g-e_g (green) exchange channels. The couplings J, Γ, and Γ' nearly vanish in the cubic limit $\Delta = 0$.

parameters, and then obtain the corresponding ground states numerically by exact diagonalization.

Exchange interactions.—In an octahedral environment, Co^{2+} ion with $t_{2g}^5 e_g^2$ configuration possesses spin $S = 3/2$ and effective orbital moment $L = 1$, which form, via spin-orbit coupling, a pseudospin $\tilde{S} = 1/2$ [14]. Over decades, cobaltates served as a paradigm for quantum magnetism, providing a variety of pseudospin-1/2 models ranging from the Heisenberg model in perovskites with corner-sharing octahedra [22,23] to the Ising model when the CoO_6 octahedra share their edges [24].

A microscopic theory of Co^{2+} interactions in the edge-sharing geometry has been developed just recently [15,16], assuming an ideal cubic symmetry. Here we consider a realistic case of trigonally distorted lattices, where t_{2g} orbitals split as shown in Fig. 2(a). Our goal is to see if such distortions leave enough room for the Kitaev model physics in real compounds. This is decided by the spin-orbital structure of the pseudospin $\tilde{S} = 1/2$ wave functions; in terms of $|S_Z, L_Z\rangle$ states (the trigonal axis $Z \| c$ is perpendicular to the honeycomb plane), they read as:

$$\left|\pm\frac{\tilde{1}}{2}\right\rangle = \mathcal{C}_1\left|\pm\frac{3}{2},\mp 1\right\rangle + \mathcal{C}_2\left|\pm\frac{1}{2},0\right\rangle + \mathcal{C}_3\left|\mp\frac{1}{2},\pm 1\right\rangle. \tag{1}$$

The coefficients $\mathcal{C}_{1,2,3}$ depend on a relative strength Δ/λ of the trigonal field $\Delta(L_Z^2 - \frac{2}{3})$ and SOC $\lambda \boldsymbol{L}\cdot\boldsymbol{S}$ [25,26]. At $\Delta = 0$, one has $(\mathcal{C}_1, \mathcal{C}_2, \mathcal{C}_3) = (1/\sqrt{2}, -1/\sqrt{3}, 1/\sqrt{6})$, and all the three components of $\boldsymbol{L}$ are equally active. A positive (negative) Δ field tends to quench L_Z ($L_{X/Y}$).

The next step is to project various spin-orbital exchange interactions in cobaltates [15] onto the above pseudospin-1/2 subspace. The calculations are standard but very lengthy; the readers interested in details are referred to the Supplemental Material [26]. At the end, we obtain the $\tilde{S} = 1/2$ Kitaev model $K\tilde{S}_i^{\gamma}\tilde{S}_j^{\gamma}$, supplemented by Heisenberg J and off-diagonal anisotropy Γ, Γ' terms; for $\gamma = z$ type NN bonds, they read as:

$$\begin{aligned}\mathcal{H}_{ij}^{(z)} = {} & K\tilde{S}_i^z\tilde{S}_j^z + J\tilde{\boldsymbol{S}}_i\cdot\tilde{\boldsymbol{S}}_j + \Gamma(\tilde{S}_i^x\tilde{S}_j^y + \tilde{S}_i^y\tilde{S}_j^x) \\ & + \Gamma'(\tilde{S}_i^x\tilde{S}_j^z + \tilde{S}_i^z\tilde{S}_j^x + \tilde{S}_i^y\tilde{S}_j^z + \tilde{S}_i^z\tilde{S}_j^y).\end{aligned} \tag{2}$$

Interactions $\mathcal{H}_{ij}^{(\gamma)}$ for $\gamma = x, y$ type bonds follow from a cyclic permutation among $\tilde{S}_j^x$, $\tilde{S}_j^y$, and $\tilde{S}_j^z$.

While the Hamiltonian (2) is of the same form as in d^5 Ir/Ru systems [5,34], the microscopic origin of its parameters K, J, Γ, Γ' is completely different in d^7 Co compounds. This is due to the spin-active e_g electrons of $Co(t_{2g}^5 e_g^2)$ ions, which generate new spin-orbital exchange

channels t_{2g}-e_g and e_g-e_g, shown in Fig. 2(b), in addition to the t_{2g}-t_{2g} ones operating in d^5 systems with t_{2g}-only electrons. In fact, the new terms make a major contribution to the exchange parameters, as illustrated in Figs. 2(c)–2(f). In particular, Kitaev coupling K comes almost entirely from the t_{2g}-e_g process. It is also noticed that t_{2g}-e_g and e_g-e_g contributions to J, Γ, and Γ' are of opposite signs and largely cancel each other, resulting in only small overall values of these couplings.

Figure 2 shows that the trigonal field Δ, which acts via modification of the pseudospin wave function (1), has an especially strong impact on the non-Kitaev couplings J, Γ, Γ'. As a result, the relative strength (J/K, etc.) of these "undesired" terms is very sensitive to Δ variations. This suggests the orbital splitting Δ as an efficient (and experimentally accessible) parameter that controls the proximity of cobaltates to the Kitaev-model regime.

Another important parameter in the theory is the U/Δ_{pd} ratio. In contrast to Ir/Ru-based Mott insulators with small $U/\Delta_{pd} \sim 0.5$, cobaltates are charge-transfer insulators [17], with typical values of $U/\Delta_{pd} \sim 2$–3 depending on the material chemistry. Including both Mott-Hubbard U and charge-transfer Δ_{pd} excitations, we have calculated [26] the exchange couplings as a function of U/Δ_{pd} and Δ/λ. Figure 3(a) shows that Kitaev coupling K is not much sensitive to U/Δ_{pd} variations. On the other hand, the non-Kitaev terms, especially Heisenberg coupling J, are quite sensitive to U/Δ_{pd}, see Figs. 3(b)–3(d). However, their values relative to K remain small over a broad range of parameters.

Phase diagram.—Having quantified the exchange parameters in Hamiltonian (2), we are now ready to address the corresponding ground states. As Kitaev coupling is the leading term, the model is highly frustrated. We therefore employ exact diagonalization (ED) which has been widely used to study phase behavior of the extended Kitaev-Heisenberg models (see, e.g., Refs. [11,35–39]). In particular, by utilizing the method of coherent spin states [38,39], we can detect and identify the magnetically ordered phases (including easy-axis directions for the ordered moments). When non-Kitaev couplings are small (roughly below 10% of the FM K value), a quantum spin-liquid state is expected. Reflecting the unique feature of the Kitaev model [1], this state is characterized by short-range spin correlations that are vanishingly small beyond nearest-neighbors [11].

The resulting phase diagram, along with the data quantifying spin correlations beyond NN distances, is presented in Figs. 3(e) and 3(f). The main trends in the phase map are easy to understand considering the variations of non-Kitaev couplings with Δ/λ and U/Δ_{pd}. As we see in Figs. 3(c) and 3(d), Γ' exactly vanishes at the $\Delta = 0$ line, and Γ is very small too. Thus, in the cubic limit, the model (2) essentially becomes the well-studied $K - J$ model, with

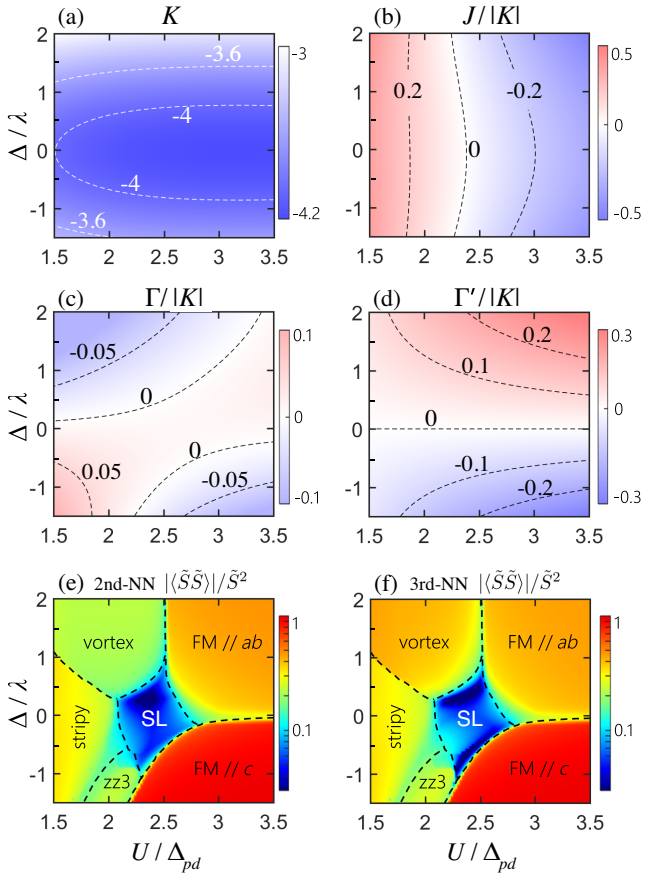

FIG. 3. (a) Kitaev coupling K (in units of t^2/U), and (b)–(d) the relative values of $J/|K|$, $\Gamma/|K|$, and $\Gamma'/|K|$ as a function of Δ/λ and U/Δ_{pd}. For convenience, specific values of parameters are indicated by contour lines. (e)–(f) The corresponding phase diagram obtained by ED of the model on a hexagon-shaped 24-site cluster. As in Fig. 1, the color maps quantify the strength of (e) second-NN and (f) third-NN spin correlations, which drop sharply in the SL phase (small but finite values are due to deviations from the pure Kitaev model [11]).

large FM Kitaev K term, and J correction changing from AF $J > 0$ to FM $J < 0$ as a function of U/Δ_{pd}. Consequently, the ground state changes from stripy AF (at small U/Δ_{pd}) to FM order at large U/Δ_{pd}, through the Kitaev SL phase in between [35]. In the SL phase, spin correlations are indeed short-ranged and bond-selective: for z-type NN bonds, we find $\langle \tilde{S}^z \tilde{S}^z \rangle / \tilde{S}^2 \simeq 0.52$ (as in the Kitaev model), while they nearly vanish at farther distances, see Figs. 3(e) and 3(f).

As we switch on the trigonal field Δ, the Γ' term comes into play confining the SL phase to the window of $|\Delta|/\lambda < 1$ (where $|\Gamma'/K| < 0.1$). In the FM phases, the sign of Γ' decides the direction of the FM moments. On the left-top (left-bottom) part of the phase map, where Heisenberg coupling J is AF, the stripy state gives way to a vortex-type [34] (zigzag-type) ordering, stabilized by the combined effect of Γ and Γ' terms.

To summarize up to now, the nearest-neighbor pseudospin Hamiltonian is dominated by the FM Kitaev model, which appears to be robust against trigonal splitting of orbitals. Subleading terms, represented mostly by J and Γ' couplings, shape the phase diagram, which includes a sizeable SL area. While these observations are encouraging, it is crucial to inspect how the picture is modified by longer range interactions, especially by the third-NN Heisenberg coupling $J_3\tilde{\mathbf{S}}_i \cdot \tilde{\mathbf{S}}_j$, which appears to be one of the major obstacles on the way to a Kitaev SL in $5d$ and $4d$ compounds [5,12]. We have no reliable estimate for J_3, since long-range interactions involve multiple exchange channels and are thus sensitive to material chemistry details. As such, they have to be determined experimentally. We note that $|J_3/K| \simeq 0.1$ was estimated [40,41] in the $4d$ compound $RuCl_3$; in cobaltates with more localized $3d$ orbitals [13], this ratio is expected to be smaller.

Adding a J_3 term to the model (2), we have reexamined the ground states and found that the Kitaev SL phase is stable up to $|J_3/K| \sim 0.06$ [26]. The modified phase diagram, obtained for a representative value of $J_3 = 0.15t^2/U \simeq 0.04|K|$, is shown in Fig. 1 [42]. Its comparison with Fig. 3 tells that the main effect of J_3 is to support the zigzag-type states (with different orientation of moments) at the expense of other phases. Note also that the SL area is shifted to the right, where FM J and AF J_3 tend to frustrate each other. The phase diagram in Fig. 1 should be generic to Co^{2+} honeycomb systems, and will be used in the following discussion.

Honeycomb lattice cobaltates.—A number of such compounds are known: $A_3Co_2SbO_6$ ($A = Na, Ag, Li$) [18–20,43,44], $Na_2Co_2TeO_6$ [18,45–47], $BaCo_2(XO_4)_2$ ($X = As$, P) [48–51], $CoTiO_3$ [52–54], $CoPS_3$ [55,56]. They are quasi-two-dimensional magnets; within the ab planes, zigzag or FM order is most common.

Traditionally, experimental data in Co^{2+} compounds is analyzed in terms of an effective $\tilde{S} = 1/2$ models of XXZ type [48,50,54,57–59]. As $\tilde{S} = 1/2$ magnons ($\sim$10 meV) are well separated from higher lying spin-orbit excitations ($\sim$30 meV), the pseudospin picture itself is well justified; however, a conventional XXZ model neglects the bond-directional nature of pseudospin $\tilde{S} = 1/2$ interactions. A general message of our work is that a proper description of magnetism in cobaltates should be based on the model of Eq. (2), supplemented by longer-range interactions. We note in passing that the XXZ model also follows from Eq. (2) when the Kitaev-type anisotropy is suppressed [34]; however, such an extreme limit is unlikely for realistic trigonal fields, given the robustness of the K coupling, see Fig. 3.

As an example, we consider $Na_3Co_2SbO_6$ which has low Néel temperature and a reduced ordered moment [20]. Analyzing the magnetic susceptibility data [20] including all spin-orbit levels [26], we obtain a positive trigonal field $\Delta \simeq 38$ meV and $\lambda \simeq 28$ meV; these values are typical for Co^{2+} ions in an octahedral environment (see, e.g., Ref. [54]). With $\Delta/\lambda \simeq 1.36$, we evaluate $\tilde{S} = 1/2$ doublet g factors $g_{ab} \simeq 4.6$ and $g_c \simeq 3$, from which a saturated moment of $2.3\mu_B$, consistent with the magnetization data [20], follows.

Zigzag-ordered moments in $Na_3Co_2SbO_6$ are confined to the ab plane [20]; this corresponds to the zz1 phase in Fig. 1. The easy-plane anisotropy is due to the Γ' term, which is positive for $\Delta > 0$, see Fig. 3(d). Regarding the location of $Na_3Co_2SbO_6$ on the U/Δ_{pd} axis of Fig. 1, we believe it is close to the FM$//ab$ phase, based on the following observations. First, a sister compound $Li_3Co_2SbO_6$ has ab-plane FM order [44] (most likely due to smaller Co-O-Co bond angle, 91° versus 93°, slightly enhancing the FM J value). Second, zigzag order gives way to fully polarized state at small magnetic fields [18,20]. These facts imply that zz1 and FM$//ab$ states are closely competing in $Na_3Co_2SbO_6$.

Based on the above considerations, we roughly locate $Na_3Co_2SbO_6$ in the phase diagram as shown in Fig. 1. In this parameter area, the exchange couplings are $K \simeq -3.6t^2/U$, $J/|K| \sim -0.14$, $\Gamma/|K| \sim -0.03$, and $\Gamma'/|K| \sim 0.16$, see Figs. 3(a)–3(d). The small values of J, Γ, Γ' imply the proximity to the Kitaev model, explaining a strong reduction of the ordered moments from their saturated values [20]. As a crucial test for our theory, we show in Fig. 4 the expected spin excitations. The large FM Kitaev interaction enhances magnon spectral weight near $\boldsymbol{q} = 0$ and leads to its anisotropy in momentum space, see Figs. 4(a) and 4(b).

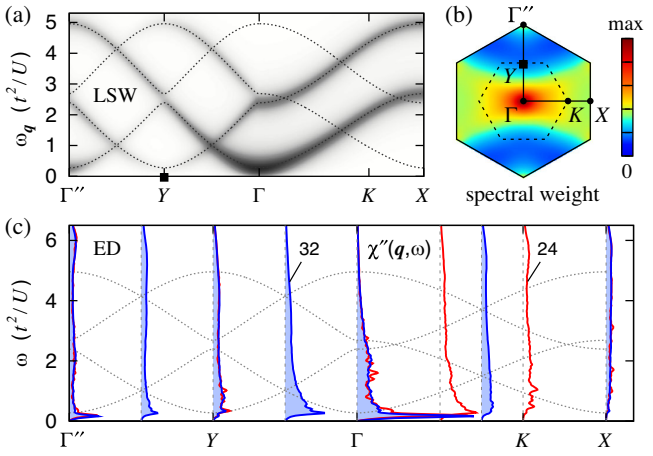

FIG. 4. Spin excitation spectrum expected in $Na_3Co_2SbO_6$. The parameters $K = -3.6$, $J = -0.5$, $\Gamma = -0.1$, $\Gamma' = 0.6$ (in units of t^2/U) follow from our theory, while $J_3 = 0.15$ is added "by hand" [63] to stabilize the zigzag order. (a) Magnon dispersions and intensities from linear spin wave (LSW) theory. (b) The energy-integrated magnon intensity over the Brillouin zone. The intensity is largest around Γ, i.e., away from the Bragg point Y. (c) Exact diagonalization results for hexagonal 24- and 32-site clusters. Plotted is the trace $\chi''(\boldsymbol{q},\omega)$ of the spin susceptibility tensor [26], which comprises the low-energy magnon peak and a broad continuum.

The ED results in Fig. 4(c) show that, as a consequence of the dominant Kitaev coupling, magnons are strongly renormalized and only survive at low energies, and a broad continuum of excitations [41,60] as in $RuCl_3$ [61,62] emerges. Neutron scattering experiments on $Na_3Co_2SbO_6$ are desired to verify these predictions.

If the above picture is confirmed by experiments, the next step should be to drive $Na_3Co_2SbO_6$ into the Kitaev SL state. As suggested by Fig. 1, this requires a reduction of the trigonal field by ∼20 meV, e.g., by means of strain or pressure control. At this point, the relative smallness of SOC for 3*d* Co ions comes as a great advantage: while strong enough to form the pseudospin moments, it makes the lattice manipulation of the $\tilde{S} = 1/2$ wave functions (and hence magnetism) far easier than in iridates [64]. Monitoring the magnetic behavior of $Na_3Co_2SbO_6$ and other honeycomb cobaltates under uniaxial pressure would be thus very interesting.

To conclude, we have presented a comprehensive theory of exchange interactions in honeycomb cobaltates, and studied their magnetic phase behavior. The analysis of $Na_3Co_2SbO_6$ data suggests that this compound is proximate to a Kitaev SL phase and could be driven there by a *c*-axis compression. A broader message is that as one goes from 5*d* Ir to 4*d* Ru and further to 3*d* Co, magnetic *d* orbitals become more localized, and this should improve the conditions for realization of the nearest-neighbor-only interaction model designed by Kitaev.

We thank A. Yaresko, T. Takayama, and A. Smerald for discussions, and M. Songvilay for sharing unpublished data. G. Kh. acknowledges support by the European Research Council under Advanced Grant No. 669550 (Com4Com). J. Ch. acknowledges support by Czech Science Foundation (GAČR) under Project No. GA19-16937S and MŠMT ČR under NPU II Project No. CEITEC 2020 (LQ1601). Computational resources were supplied by the Project "e-Infrastruktura CZ" (No. e-INFRA LM2018140) provided within the program Projects of Large Research, Development and Innovations Infrastructures.

[1] A. Kitaev, Ann. Phys. (N.Y.) **321**, 2 (2006).
[2] L. Savary and L. Balents, Rep. Prog. Phys. **80**, 016502 (2017).
[3] M. Hermanns, I. Kimchi, and J. Knolle, Annu. Rev. Condens. Matter Phys. **9**, 17 (2018).
[4] S. Trebst, arXiv:1701.07056.
[5] S. M. Winter, A. A. Tsirlin, M. Daghofer, J. van den Brink, Y. Singh, P. Gegenwart, and R. Valentí, J. Phys. Condens. Matter **29**, 493002 (2017).
[6] H. Takagi, T. Takayama, G. Jackeli, G. Khaliullin, and S. E. Nagler, Nat. Rev. Phys. **1**, 264 (2019).
[7] Y. Motome and J. Nasu, J. Phys. Soc. Jpn. **89**, 012002 (2020).
[8] G. Khaliullin, Prog. Theor. Phys. Suppl. **160**, 155 (2005).
[9] G. Jackeli and G. Khaliullin, Phys. Rev. Lett. **102**, 017205 (2009).
[10] K. W. Plumb, J. P. Clancy, L. J. Sandilands, V. V. Shankar, Y. F. Hu, K. S. Burch, H.-Y. Kee, and Y.-J. Kim, Phys. Rev. B **90**, 041112(R) (2014).
[11] J. Chaloupka, G. Jackeli, and G. Khaliullin, Phys. Rev. Lett. **105**, 027204 (2010).
[12] S. M. Winter, Y. Li, H. O. Jeschke, and R. Valentí, Phys. Rev. B **93**, 214431 (2016).
[13] Cf. $\langle r^2 \rangle_{3d} = 1.25$ and $\langle r^2 \rangle_{4d} = 2.31$ for Co^{2+} and Ru^{3+} ions (in a.u.), respectively [14].
[14] A. Abragam and B. Bleaney, *Electron Paramagnetic Resonance of Transition Ions* (Clarendon Press, Oxford, 1970).
[15] H. Liu and G. Khaliullin, Phys. Rev. B **97**, 014407 (2018).
[16] R. Sano, Y. Kato, and Y. Motome, Phys. Rev. B **97**, 014408 (2018).
[17] J. Zaanen, G. A. Sawatzky, and J. W. Allen, Phys. Rev. Lett. **55**, 418 (1985).
[18] L. Viciu, Q. Huang, E. Morosan, H. W. Zandbergen, N. I. Greenbaum, T. McQueen, and R. J. Cava, J. Solid State Chem. **180**, 1060 (2007).
[19] C. Wong, M. Avdeev, and C. D. Ling, J. Solid State Chem. **243**, 18 (2016).
[20] J.-Q. Yan, S. Okamoto, Y. Wu, Q. Zheng, H. D. Zhou, H. B. Cao, and M. A. McGuire, Phys. Rev. Mater. **3**, 074405 (2019).
[21] S. I. Csiszar, M. W. Haverkort, Z. Hu, A. Tanaka, H. H. Hsieh, H.-J. Lin, C. T. Chen, T. Hibma, and L. H. Tjeng, Phys. Rev. Lett. **95**, 187205 (2005).
[22] T. M. Holden, W. J. L. Buyers, E. C. Svensson, R. A. Cowley, M. T. Hutchings, D. Hukin, and R. W. H. Stevenson, J. Phys. C **4**, 2127 (1971).
[23] W. J. L. Buyers, T. M. Holden, E. C. Svensson, R. A. Cowley, and M. T. Hutchings, J. Phys. C **4**, 2139 (1971).
[24] R. Coldea, D. A. Tennant, E. M. Wheeler, E. Wawrzynska, D. Prabhakaran, M. Telling, K. Habicht, P. Smeibidl, and K. Kiefer, Science **327**, 177 (2010).
[25] M. E. Lines, Phys. Rev. **131**, 546 (1963).
[26] See the Supplemental Material at http://link.aps.org/supplemental/10.1103/PhysRevLett.125.047201 for Co^{2+} ionic wave functions, computational details of the exchange couplings and phase diagrams, spin excitation spectra, and the analysis of experimental data in $Na_3Co_2SbO_6$, which includes Refs. [27–33].
[27] G. W. Pratt, Jr. and R. Coelho, Phys. Rev. **116**, 281 (1959).
[28] V. I. Anisimov, J. Zaanen, and O. K. Andersen, Phys. Rev. B **44**, 943 (1991).
[29] W. E. Pickett, S. C. Erwin, and E. C. Ethridge, Phys. Rev. B **58**, 1201 (1998).
[30] H. Jiang, R. I. Gomez-Abal, P. Rinke, and M. Scheffler, Phys. Rev. B **82**, 045108 (2010).
[31] K. Foyevtsova, H. O. Jeschke, I. I. Mazin, D. I. Khomskii, and R. Valentí, Phys. Rev. B **88**, 035107 (2013).
[32] J. Chaloupka and G. Khaliullin, Prog. Theor. Phys. Suppl. **176**, 50 (2008).
[33] S. H. Chun, J.-W. Kim, Jungho Kim, H. Zheng, C. C. Stoumpos, C. D. Malliakas, J. F. Mitchell, K. Mehlawat, Y. Singh, Y. Choi, T. Gog, A. Al-Zein, M. Moretti Sala,

M. Krisch, J. Chaloupka, G. Jackeli, G. Khaliullin, and B. J. Kim, Nat. Phys. **11**, 462 (2015).
[34] J. Chaloupka and G. Khaliullin, Phys. Rev. B **92**, 024413 (2015).
[35] J. Chaloupka, G. Jackeli, and G. Khaliullin, Phys. Rev. Lett. **110**, 097204 (2013).
[36] S. Okamoto, Phys. Rev. Lett. **110**, 066403 (2013).
[37] J. G. Rau, Eric Kin-Ho Lee, and H.-Y. Kee, Phys. Rev. Lett. **112**, 077204 (2014).
[38] J. Chaloupka and G. Khaliullin, Phys. Rev. B **94**, 064435 (2016).
[39] J. Rusnačko, D. Gotfryd, and J. Chaloupka, Phys. Rev. B **99**, 064425 (2019).
[40] S. M. Winter, K. Riedl, D. Kaib, R. Coldea, and R. R. Valentí, Phys. Rev. Lett. **120**, 077203 (2018).
[41] S. M. Winter, K. Riedl, P. A. Maksimov, A. L. Chernyshev, A. Honecker, and R. R. Valentí, Nat. Commun. **8**, 1152 (2017).
[42] In Fig. 1, the Δ/λ axis of Fig. 3 is replaced by Δ, using $\lambda = 28$ meV for Co^{2+} ion.
[43] E. A. Zvereva, M. I. Stratan, A. V. Ushakov, V. B. Nalbandyan, I. L. Shukaev, A. V. Silhanek, M. Abdel-Hafiez, S. V. Streltsov, and A. N. Vasiliev, Dalton Trans. **45**, 7373 (2016).
[44] M. I. Stratan, I. L. Shukaev, T. M. Vasilchikova, A. N. Vasiliev, A. N. Korshunov, A. I. Kurbakov, V. B. Nalbandyan, and E. A. Zvereva, New J. Chem. **43**, 13545 (2019).
[45] E. Lefrançois, M. Songvilay, J. Robert, G. Nataf, E. Jordan, L. Chaix, C. V. Colin, P. Lejay, A. Hadj-Azzem, R. Ballou, and V. Simonet, Phys. Rev. B **94**, 214416 (2016).
[46] A. K. Bera, S. M. Yusuf, A. Kumar, and C. Ritter, Phys. Rev. B **95**, 094424 (2017).
[47] W. Yao and Y. Li, Phys. Rev. B **101**, 085120 (2020).
[48] L. P. Regnault, C. Boullier, and J. Y. Henry, Physica (Amsterdam) **385B**, 425 (2006).
[49] R. Zhong, T. Gao, N. P. Ong, and R. J. Cava, Sci. Adv. **6**, eaay6953 (2020).
[50] H. S. Nair, J. M. Brown, E. Coldren, G. Hester, M. P. Gelfand, A. Podlesnyak, Q. Huang, and K. A. Ross, Phys. Rev. B **97**, 134409 (2018).
[51] R. Zhong, M. Chung, T. Kong, L. T. Nguyen, S. Lei, and R. J. Cava, Phys. Rev. B **98**, 220407(R) (2018).
[52] R. E. Newnham, J. H. Fang, and R. P. Santoro, Acta Crystallogr. **17**, 240 (1964).
[53] A. M. Balbashov, A. A. Mukhin, V. Y. Ivanov, L. D. Iskhakova, and M. E. Voronchikhina, Low Temp. Phys. **43**, 965 (2017).
[54] B. Yuan, I. Khait, G.-J. Shu, F. C. Chou, M. B. Stone, J. P. Clancy, A. Paramekanti, and Y.-J. Kim, Phys. Rev. X **10**, 011062 (2020).
[55] R. Brec, Solid State Ionics **22**, 3 (1986).
[56] A. R. Wildes, V. Simonet, E. Ressouche, R. Ballou, and G. J. McIntyre, J. Phys. Condens. Matter **29**, 455801 (2017).
[57] M. T. Hutchings, J. Phys. C **6**, 3143 (1973).
[58] K. Tomiyasu, M. K. Crawford, D. T. Adroja, P. Manuel, A. Tominaga, S. Hara, H. Sato, T. Watanabe, S. I. Ikeda, J. W. Lynn, K. Iwasa, and K. Yamada, Phys. Rev. B **84**, 054405 (2011).
[59] K. A. Ross, J. M. Brown, R. J. Cava, J. W. Krizan, S. E. Nagler, J. A. Rodriguez-Rivera, and M. B. Stone, Phys. Rev. B **95**, 144414 (2017).
[60] M. Gohlke, R. Verresen, R. Moessner, and F. Pollmann, Phys. Rev. Lett. **119**, 157203 (2017).
[61] A. Banerjee, P. Lampen-Kelley, J. Knolle, C. Balz, A. A. Aczel, B. Winn, Y. Liu, D. Pajerowski, J. Yan, C. A. Bridges, A. T. Savici, B. C. Chakoumakos, M. D. Lumsden, D. A. Tennant, R. Moessner, D. G. Mandrus, and S. E. Nagler, npj Quantum Mater. **3**, 8 (2018).
[62] L. J. Sandilands, Y. Tian, K. W. Plumb, Y.-J. Kim, and K. S. Burch, Phys. Rev. Lett. **114**, 147201 (2015).
[63] In fact, the choice of J_3 is dictated by the close proximity of zz1 and FM$//ab$ states in $Na_3Co_2SbO_6$. Classically, they differ by $J - \Gamma + 3J_3$; this gives a rough idea of $J_3 \sim -J/3$ (as Γ is very small).
[64] H. Liu and G. Khaliullin, Phys. Rev. Lett. **122**, 057203 (2019).